HHS Public Access

Author manuscript

ACS Biomater Sci Eng. Author manuscript; available in PMC 2021 September 30.

Published in final edited form as:

ACS Biomater Sci Eng. 2020 September 14; 6(9): 4851–4857. doi:10.1021/acsbiomaterials.0c01047.

Gap Junction Liposomes for Efficient Delivery of Chemotherapeutics to Solid Tumors

Andrea N. Trementozzi[a], **Stephanie Hufnagel**[b], **Haiyue Xu**[b], **Mahmoud S. Hanafy**[b], **Felipe Rosero Castro**[a], **Hugh D.C. Smyth**[b], **Zhengrong Cui**[b], **Jeanne C. Stachowiak**[a,*]

[a]Department of Biomedical Engineering, The University of Texas at Austin;

[b]College of Pharmacy, The University of Texas at Austin.

Abstract

Chemotherapeutic delivery is limited by inefficient transport across cellular membranes. Here, we harness the cellular gap junction network to release therapeutic cargos directly into the cytosol. Specifically, cell-derived vesicles, termed Connectosomes, contain gap junction transmembrane proteins that open a direct passageway to the cellular interior. Connectosomes were previously shown to substantially improve chemotherapeutic delivery *in vitro*. Here, we test Connectosomes *in vivo*, using a murine breast tumor model. We demonstrate that Connectosomes improve chemotherapeutic delivery to cellular targets within tumors by up to 16-fold, compared to conventional drug-loaded liposomes, suggesting an efficient alternative pathway for intracellular delivery.

Graphical Abstract

*To whom correspondence should be addressed: Jeanne Stachowiak (jcstach@austin.utexas.edu).

AUTHOR CONTRIBUTIONS

All authors designed and performed experiments. In addition, all authors consulted together on the interpretation of results and the preparation of the manuscript.

COMPETING INTERESTS

The authors declare no competing interest.

SUPPORTING INFORMATION

More details regarding materials and methods can be found in supporting materials.

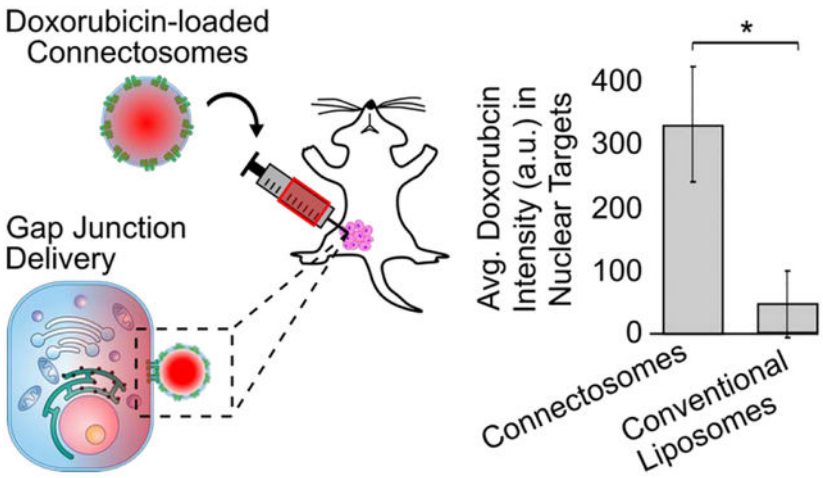

Keywords

Gap junction channels; delivery; intracellular; intratumoral; murine mammary tumor

During the past three decades, nanoparticle systems for drug delivery have been developed with the goal of improving the pharmacokinetics and biodistribution of chemotherapeutics.[1, 2] Nanoparticles possess several advantages over unencapsulated drugs, including increased circulation time in the blood stream, improved localization within tumors, and reduced toxicity.[3–6] Despite these advantages, there are still significant barriers to efficient delivery and release of drugs within tumor cells.[7] First, overcoming the plasma membrane to enter cells and reach intracellular targets remains a challenge for many nanoparticles. Specifically, most particles enter cells by endocytosis, where entrapment within endosomes prevents the release of drug cargo and limits intracellular bioavailability.[1, 8, 9] Second, nanoparticles themselves, which are optimized for stable drug encapsulation, can pose a barrier to efficient release, limiting bioavailability of the drug within tumor cells.[3, 10–13] For example, the commercial form of liposomal doxorubicin, DOXIL, increases the half-life of doxorubicin in circulation and reduces its cardiac toxicity.[14] However, poor drug release from liposomes, even once internalized within tumor cells, inhibits their therapeutic performance.[12, 14, 15]

Towards the goal of improving intracellular delivery from nanoparticles, we have developed Connectosomes, lipid vesicles that harness the gap junction network to deliver drug molecules into the cellular interior.[16] Gap junctions, protein channels that form between neighboring cells throughout the body, allow the passage of small molecules, siRNAs, and peptides from the interior of one cell directly into the interior of its neighbors.[17, 18] Gap junctions are comprised of the transmembrane protein, connexin, which forms hexamers, called connexons, on the plasma membrane. In addition to healthy cells, these connexin proteins are also found in many cancer cells, including breast tumors.[19] From a therapeutic perspective, gap junction channels in tumor tissue have been shown to facilitate intercellular diffusion of drug molecules to improve the anti-tumor effects of chemotherapeutics.[20–22] Furthermore, we have previously demonstrated that gap junction-mediated delivery via

Connectosomes substantially reduces the therapeutically effective dose of doxorubicin, *in vitro*.[16] Connectosomes contain connexin proteins in their membrane, which allows them to form functional gap junctions with tumor cells of interest, providing a direct pathway for delivery. These results provide a foundation for our current efforts, which aim to evaluate the performance of Connectosomes for gap junction-mediated delivery to tumor cells *in vivo*.

Here, we compare the *in vivo* performance of doxorubicin-loaded Connectosomes to that of DOXIL, by directly injecting each of them into mammary tumors transplanted in C57BL/6 mice. Our data demonstrate that using Connectosomes to deliver doxorubicin increases localization of the drug to tumor cell nuclear targets by as much as 16-fold in comparison to delivery of the same dose using DOXIL. These data suggest that, by harnessing the cellular gap junction network, Connectosomes have the potential to substantially improve intracellular delivery of chemotherapeutics relative to existing liposomal formulations.

We chose retinal pigmented epithelial (RPE) cells, which express high endogenous levels of connexin 43,[23–25] as the donor cell line for Connectosomes. To evaluate gap junction functionality of RPE cells, we used a scratch loading assay[26], which provides a rapid and direct method for assessing gap junction intercellular communication between cells. HeLa cells, which are known to have low gap junction-mediated cell-to-cell communication[27], provided a negative control for these studies (Figures 1A, 1B). Once either RPE or HeLa cells were plated and grown to confluency, a pipet tip containing Lucifer yellow CH dye was scraped through the monolayer of cells to create a scratch. Dye was simultaneously dispensed throughout the scratch to load the newly damaged cells, and cells were incubated for 5 minutes at 37°C to allow dye transfer to occur. Since Lucifer yellow dye is impermeable to cell membranes, transfer of dye from the scratched cells to undamaged, neighboring cells is expected to occur through gap junction channels.[26] Therefore, we expect a gradient of dye concentration from the scratch into the surrounding cells. For cells with increased gap junction communication, the gradient should occur over a longer distance. As expected, a gradient in dye concentration was detected upon scratching RPE cells with Lucifer yellow dye (Figure 1A). Here, 40% of the initial dye fluorescence was detected about 100 μm from the scratch (Figure 1A). In contrast, HeLa cells exhibited an abrupt drop in dye fluorescence as we moved away from the scratch, with only about 2% of the initial dye detectable 100 μm from the scratch (Figure 1B).

To verify that dye transfer was occurring through gap junction channels and not by an alternative mechanism, we also performed the scratch loading assay in the presence of carbenoxolone (CBX), a known gap junction inhibitor.[28] Here confluent monolayers of RPE cells and HeLa cells were each incubated with 100 μM of CBX at 37°C for at least 30 minutes prior to conducting the scratch loading assay. Here the dye concentration gradient was substantially reduced (Figure 1A), with only 3% of the initial fluorescence detected at 100 μm from the scratch. Sensitivity of dye transfer to the presence of CBX indicates that functional gap junctions exist between the RPE cells. Notably, at a similar distance from the scratch, dye intensity in HeLa cells remained near 2% in the presence of CBX, almost identical to results without the gap junction inhibitor (Figure 1B). This lack of sensitivity indicates that HeLa cells lack a well-established gap junction network, as expected.

Once gap junction functionality was characterized, we generated Connectosomes by extracting giant plasma membrane vesicles (GPMVs) from RPE donor cells, using a cellular membrane blebbing process (see Supporting Information, Figure 1C).[29, 30] This blebbing process is known to retain transmembrane protein orientation and function.[29] Extracted vesicles reveal a similar morphology to other lipid vesicles,[31] and they average about 10 μm in diameter.[16] To visualize Connectosomes, donor cells expressed the transmembrane domain of the transferrin receptor fused to an extracellular blue fluorescent protein (TfR-BFP). Fluorescence signal from TfR-BFP was evident in vesicles budding from donor cells (Figure 1C) and in Connectosomes (Figure 1D).

To evaluate the functionality of connexon hemichannels within Connectosomes, we examined the ability of calcium to control the permeability of the membranes to fluorescent dyes (Figure 1D). Millimolar levels of calcium cause connexon hemichannels to close,[32] preventing the passage of molecules across membranes. To test hemichannel functionality, donor cells were incubated with calcein red-orange (CRO) acetomethoxy (AM) dye and subsequently blebbed to extract Connectosomes filled with CRO dye (see methods). Once loaded into the vesicles, the dye was impermeable to the membrane due to hydrolysis of the acetomethoxy group. Thus, CRO dye molecules were trapped within Connectosomes and could only exit through open gap junction channels. When calcium was present at a concentration of 2 mM in the surrounding solution, CRO dye was retained within Connectosomes (Figure 1D). However, upon removal of calcium from the solution using 5 mM of ETDA (ethylenediaminetetraacetic acid) and EGTA (ethylene glycol tetraacetic acid), both calcium chelators, we observed the release of CRO dye from Connectosomes (Figure 1D). Flow cytometry further demonstrated dye release from Connectosomes as seen by a leftward shift in the CRO dye fluorescence intensity histogram when chelators were introduced (Figure 1E). Here the median fluorescence intensity of CRO dye was reduced by about 64% compared to the condition in which chelators were absent.

Having established that Connectosome vesicles contain functional connexon hemichannels, we next sought to encapsulate doxorubicin. First, we explored a passive loading mechanism that was used previously.[33] Here, Connectosomes were resuspended in a solution containing 1 mg/mL of doxorubicin and subsequently extruded through a filter with 100 nm diameter pores. The extrusion process disrupted the Connectosome membrane, allowing passive diffusion of doxorubicin into the vesicles (Figure 2A). Unencapsulated doxorubicin was removed using a centrifugal filter (see Supporting Information). Dynamic light scattering (DLS) measurements indicated that the number average diameter for doxorubicin-loaded Connectosomes was 52 ± 6 nm. We quantified doxorubicin loading of Connectosomes by measuring their absorbance at 480 nm (see Supporting Information, Figure S1).[34, 35] With this passive mechanism of loading, we were able to retain about 15% of the drug within Connectosomes (Figure 2C), as determined by calculating the fraction of initial doxorubicin remaining after removing unencapsulated drug by filtration.

To increase the encapsulation of drugs within Connectosomes, we next explored an active doxorubicin loading method, well documented in the formulation of DOXIL.[3] This method leverages a transmembrane ammonium sulfate gradient to drive accumulation of doxorubicin within liposomes (see Supporting Information, Figure 2B).[10, 36] Here Connectosomes were

resuspended in an ammonium sulfate solution, pH 5.4, and extruded through a filter with a 100 nm average pore diameter. Extrusion enables incorporation of the low pH solution within the Connectosomes. The vesicles were then dialyzed in a neutral buffer (10 mM HEPES, 2 mM $CaCl_2$, 150 mM NaCl, pH 7.4) to remove unincorporated ammonium sulfate. Then Connectosomes were incubated in a solution containing 1 mg/mL of doxorubicin for one hour at 37°C to achieve encapsulation of the drug. During this incubation period, membrane permeable doxorubicin is expected to diffuse into the Connectosome where it should become protonated and form aggregates with sulfate ions, substantially reducing its membrane permeability.[36] After one hour of incubation with doxorubicin, unencapsulated drug was removed by centrifugal filtration. DLS indicated a modest increase in number average diameter associated with doxorubicin loading (75 ± 16 nm versus 99 ± 28 nm). Using this protocol, Connectosomes retained 42% of the initial drug, on average, relating to a 3-fold improvement over the passive loading protocol (Figure 2C).

Next, we compared the cellular uptake of doxorubicin upon its delivery by either Connectosomes or DOXIL. Doxorubicin targets the cellular nuclei, where it disrupts DNA-associated enzymes and intercalates with DNA base-pairs to prevent transcription.[37] To detect whether or not doxorubicin reached its target, we evaluated its fluorescence within cell nuclei. In these experiments we exposed confluent monolayers of HeLa cells to either doxorubicin-loaded Connectosomes or DOXIL. Notably, HeLa cells do not have strong connexin activity in comparison to RPE cells. However, we have previously demonstrated that HeLa cells have sufficient connexin expression to facilitate gap-junction dependent drug delivery.[16, 33] For each treatment, 12 μg of doxorubicin, loaded within DOXIL or within Connectosomes, was incubated with cells in 200 μL total volumes. Two hours after exposure to the treatment, the cells were imaged to detect doxorubicin fluorescence using a spinning disc confocal fluorescence microscope. For each treatment group, doxorubicin fluorescence was visible in the HeLa cell nuclei. However, the fluorescence of doxorubicin was considerably reduced for HeLa cells treated with DOXIL, compared to those treated with doxorubicin-loaded Connectosomes (Figure 2D). Quantification by flow cytometry revealed more than a 5-fold increase in median doxorubicin fluorescence intensity within cells after two hours of incubation with doxorubicin-loaded Connectosomes compared to DOXIL (Figure 2E). We also examined cellular uptake of unencapsulated, free doxorubicin (12 μg) added directly to the culture medium. Flow cytometry data revealed that doxorubicin fluorescence was 1.2-fold brighter in cells treated with doxorubicin-loaded Connectosomes compared to cells treated with the free drug (Figure 2E). These results suggest that Connectosomes are more efficient at delivering doxorubicin to cellular nuclei when compared to conventional liposomal doxorubicin and unencapsulated doxorubicin.

A mammary tumor mouse model was used to evaluate the extent to which Connectosomes can improve doxorubicin delivery to tumor cells *in vivo*. Mesenchymal-Wnt (M-Wnt) cells[38], which demonstrate high gap junction functionality (Supplementary Figure S2), were used to generate the mammary tumor. M-Wnt cells were injected into the fourth mammary fat pad of nine C57BL/6 mice at 1×10^6 cells/mouse (Figure 3A). After mammary tumors measured approximately 4 – 7 mm in diameter, we delivered the doxorubicin treatments by intratumoral injection (Figure 3A), as none of the delivery vehicles contained targeting ligands. Doxorubicin-loaded Connectosomes, at a dose of 0.5 mg of doxorubicin per

kilogram of body weight, were injected into the tumors of three mice. DOXIL, also at 0.5 mg/kg of doxorubicin, was injected into the tumors of a second group of three mice. Finally, a third group of three mice were left untreated. Two hours after injections, all mice were sacrificed for tumor extraction and analysis.

Confocal fluorescence imaging of mammary tumor slices revealed that doxorubicin fluorescence within tumors from mice treated with doxorubicin-loaded Connectosomes was brighter compared to tumors treated with DOXIL (Figure 3B, 3D). Notably, doxorubicin fluorescence from the tumors of mice treated with Connectosomes appeared to colocalize distinctly with DAPI staining, suggesting that doxorubicin reached tumor cell nuclei, its intracellular target.[39] In contrast, tumors treated with DOXIL display a more diffuse doxorubicin signal that did not appear to colocalize as distinctly with nuclear DAPI staining (Figure 3D).

Quantifying nuclear doxorubicin intensity across full tumor sections confirmed a shift of the intensity distribution toward higher values for Connectosome treatment compared to DOXIL treatment (Figure 3C). Examining the average nuclear doxorubicin fluorescence intensity for all tumors treated with Connectosomes and for all tumors treated with DOXIL shows that the nuclear fluorescence intensity of doxorubicin delivered by Connectosomes was about 7-fold greater than that delivered by DOXIL, $p < 0.05$ (Figure 3C).

We further sought to quantify nuclear doxorubicin fluorescence from the region containing the brightest doxorubicin signal within each tumor, close to the sites of injection (Figures 3D, 3E). Areas distant from the site of injection were unlikely to receive a substantial dose of doxorubicin, making it more difficult to assess the potential benefits of one delivery system compared to the other. As expected, plotting the distribution of nuclear doxorubicin fluorescence intensity within the brightest regions revealed a larger, 16-fold difference in fluorescence intensity between tumors injected with Connectosomes and tumors injected with DOXIL, $p < 0.05$ (Figure 3E). These data reveal that significantly less doxorubicin is localized to nuclear targets in tumors injected with DOXIL, in comparison to tumors injected with Connectosomes, two hours post treatment. Possible reasons for the more cytosolic distribution of doxorubicin in tumors injected with DOXIL include persistent entrapment of doxorubicin within liposomes[12], or entrapment of the liposomes within endosomes following their uptake by cells.[8] Collectively, these results demonstrate that connectosomes are more effective in the rapid delivery of doxorubicin to tumor cell nuclei, in comparison to DOXIL.

Here we have used a murine mammary tumor model to test the ability of Connectosomes to deliver the chemotherapeutic, doxorubicin, *in vivo*. Connectosomes are cell-derived membrane vesicles that use the gap junction network to deliver encapsulated therapeutics directly into the cytoplasm. We extracted Connectosomes from RPE cells, which exhibit high levels of endogenous connexin expression. Results from a scratch loading assay confirmed that RPE cells exhibited high gap junction functionality (Figures 1A, 1B). We further demonstrated that Connectosomes extracted from RPE cells exhibit calcium-dependent retention of encapsulated dye molecules, confirming their gap junction functionality (Figures 1D and 1E).

After characterizing Connectosomes extracted from RPE donor cells, we optimized loading of the chemotherapeutic doxorubicin within these vesicles. By introducing a transmembrane ammonium sulfate gradient during the drug loading process, we obtained a 3-fold increase in the fraction of drug encapsulated (Figure 2C). In *in vitro* studies, Connectosomes substantially enhanced the delivery of doxorubicin to cellular nuclei compared to DOXIL (Figures 2D, 2E). Finally, we delivered Connectosomes to tumors in C57BL/6 mice by intratumoral injection. Results, two hours after injection, revealed up to a 16-fold increase in nuclear doxorubicin signal in tumors receiving Connectosomes, compared to tumors receiving DOXIL (Figures 3B – 3E).

Previous studies on intracellular uptake of DOXIL report that doxorubicin transport to the cellular nuclei is slow and inefficient, with less than 1% of the drug entering the nuclei after 8 hours.[12] The slow release of doxorubicin from DOXIL helps to concentrate the drug within tumors by increasing its circulation time.[3] However, release is often so slow that even when internalized into cells by endocytosis, doxorubicin often remains trapped within the vesicles, preventing efficient release and transport to drug targets.[15] Toward addressing this barrier, we observe increased transport of doxorubicin to cellular nuclei when using Connectosomes for delivery, both *in vitro* and *in vivo*. Increasing drug transport leads to greater intracellular drug accumulation, suggesting the potential to overcome reverse transport mechanisms, such as efflux pumps,[40] which presently limit drug effectiveness. Next steps include evaluating the anti-tumor effects of doxorubicin-loaded Connectosomes upon intravenous injection. Further, we are evaluating the ability of Connectosomes to deliver a broader range of therapeutic molecules, including small interfering RNAs (siRNAs) for knockdown of tumor-promoting genes.

Connectosomes provide a direct pathway for delivering therapeutic cargo to the cytosol, creating the potential to overcome the limitations of traditional vehicles, which are internalized by endocytosis.[9] Our results suggest that Connectosomes have the potential to enhance delivery and intracellular release of drugs, improving upon existing liposomal formulations.

Supplementary Material

Refer to Web version on PubMed Central for supplementary material.

ACKNOWLEDGEMENTS

This research was supported through the National Institute of Health through grant R21EB025490 to Stachowiak and Smyth.

REFERENCES

1. Blanco E; Shen H; Ferrari M, Principles of nanoparticle design for overcoming biological barriers to drug delivery. Nat Biotechnol2015, 33 (9), 941–51. [PubMed: 26348965]
2. Wang AZ; Langer R; Farokhzad OC, Nanoparticle Delivery of Cancer Drugs. 10.1146/annurev-med-040210-1625442012, 63, 185–198.
3. Barenholz Y, Doxil(R)--the first FDA-approved nano-drug: lessons learned. J Control Release2012, 160 (2), 117–34. [PubMed: 22484195]

4. Ragelle H; Danhier F; Préat V; Langer R; Anderson DG, Nanoparticle-based drug delivery systems: a commercial and regulatory outlook as the field matures. 10.1080/17425247.2016.12441872016, 14 (7), 851–864.
5. Tran S; DeGiovanni PJ; Piel B; Rai P, Cancer nanomedicine: a review of recent success in drug delivery. Clin Transl Med2017, 6 (1), 44. [PubMed: 29230567]
6. Wolinsky JB; Colson YL; Grinstaff MW, Local drug delivery strategies for cancer treatment: gels, nanoparticles, polymeric films, rods, and wafers. J Control Release2012, 159 (1), 14–26. [PubMed: 22154931]
7. De Jong WH; Borm PJA, Drug delivery and nanoparticles: Applications and hazards. International Journal of Nanomedicine2008, 3 (2), 133–149. [PubMed: 18686775]
8. Kou L; Sun J; Zhai Y; He Z, The endocytosis and intracellular fate of nanomedicines: Implication for rational design. Asian Journal of Pharmaceutical Sciences2013, 8 (1), 1–10.
9. Sahay G; Alakhova DY; Kabanov AV, Endocytosis of nanomedicines. J Control Release2010, 145 (3), 182–95. [PubMed: 20226220]
10. Haran G; Cohen R; Bar LK; Barenholz Y, Transmembrane ammonium sulfate gradients in liposomes produce efficient and stable entrapment of amphipathic weak bases. Biochimica et Biophysica Acta (BBA) - Biomembranes1993, 1151 (2), 201–215. [PubMed: 8373796]
11. Lasic DD; Čeh B; Stuart MCA; Guo L; Frederik PM; Barenholz Y, Transmembrane gradient driven phase transitions within vesicles: lessons for drug delivery. Biochimica et Biophysica Acta (BBA) - Biomembranes1995, 1239 (2), 145–156. [PubMed: 7488619]
12. Seynhaeve ALB; Dicheva BM; Hoving S; Koning GA; Ten Hagen TLM, Intact Doxil is taken up intracellularly and released doxorubicin sequesters in the lysosome: evaluated by in vitro/in vivo live cell imaging. J Control Release2013, 172 (1), 330–340. [PubMed: 24012486]
13. Gradishar WJ; Tjulandin S; Davidson N; Shaw H; Desai N; Bhar P; Hawkins M; O'Shaughnessy J, Phase III trial of nanoparticle albumin-bound paclitaxel compared with polyethylated castor oil-based paclitaxel in women with breast cancer. J Clin Oncol2005, 23 (31), 7794–803. [PubMed: 16172456]
14. O'Brien ME; Wigler N; Inbar M; Rosso R; Grischke E; Santoro A; Catane R; Kieback DG; Tomczak P; Ackland SP; Orlandi F; Mellars L; Alland L; Tendler C, Reduced cardiotoxicity and comparable efficacy in a phase III trial of pegylated liposomal doxorubicin HCl (CAELYX/Doxil) versus conventional doxorubicin for first-line treatment of metastatic breast cancer. Ann Oncol2004, 15 (3), 440–9. [PubMed: 14998846]
15. Laginha KM; Verwoert S; Charrois GJR; Allen TM, Determination of Doxorubicin Levels in Whole Tumor and Tumor Nuclei in Murine Breast Cancer Tumors. Clinical Cancer Research2005, 11 (19), 6944–6949. [PubMed: 16203786]
16. Gadok AK; Busch DJ; Ferrati S; Li B; Smyth HDC; Stachowiak JC, Connectosomes for Direct Molecular Delivery to the Cellular Cytoplasm. Journal of the American Chemical Society2016, 138 (39), 12833–12840. [PubMed: 27607109]
17. Goodenough DA; Paul DL, Gap Junctions. Cold Spring Harbor Perspectives in Biology2009, 1 (1), a002576. [PubMed: 20066080]
18. Gulistan Mese GR, Thomas WWhite, Gap Junctions: Basic Structure and Function. Journal of Investigative Dermatology2007, 127 (11), 2516–2524.
19. Maksim Sinyuk EEM-H, Reizes Ofer, Lathia Justin, Cancer Connectors: Connexins, Gap Junctions, and Communication. Frontiers in Oncology2018, 8 (646).
20. Ding Y; Nguyen TA, Gap Junction Enhancer Potentiates Cytotoxicity of Cisplatin in Breast Cancer Cells. J Cancer Sci Ther2012, 4 (11), 371–8. [PubMed: 25045421]
21. Zhang Y; Tao L; Fan L; Peng Y; Yang K; Zhao Y; Song Q; Wang Q, Different gap junction-propagated effects on cisplatin transfer result in opposite responses to cisplatin in normal cells versus tumor cells. Sci Rep2015, 5.
22. Cottin S; Ghani K; Campos-Lima P. O. d.; Caruso M, Gemcitabine intercellular diffusion mediated by gap junctions: new implications for cancer therapy. Molecular Cancer2010, 9 (1), 1–10. [PubMed: 20051109]
23. Akanuma S; Higashi H; Maruyama S; Murakami K; Tachikawa M; Kubo Y; Hosoya K, Expression and function of connexin 43 protein in mouse and human retinal pigment epithelial cells as

hemichannels and gap junction proteins. - PubMed - NCBI.Experimental Eye Research2018, (168), 128–137.

24. Tibber M; Becker D; Jeffery G, Levels of transient gap junctions between the retinal pigment epithelium and the neuroblastic retina are influenced by catecholamines and correlate… - PubMed - NCBI. Journal of Comparative Neurology 2007, 1 (503), 128–134.
25. Calera M; Topley H; Liao Y; Duling B; Paul D; Goodenough D, Connexin43 is required for production of the aqueous humor in the murine eye. - PubMed - NCBI.Journal of Cell Science2006, 119, 4510–4519. [PubMed: 17046998]
26. el-Fouly M; Trosko J; Chang C, Scrape-loading and dye transfer. A rapid and simple technique to study gap junctional intercellular communication. - PubMed - NCBI.Experimental Cell Research1987, 2 (168), 422–430.
27. Eckert R; Dunina-Barkovskaya A; Hüsler D, Biophysical characterization of gap-junction channels in HeLa cells. - PubMed - NCBI.Pflügers Archive1993, 424, 335–342. [PubMed: 7692394]
28. Davidson JS; Baumgarten IM; Harley EH, Reversible inhibition of intercellular junctional communication by glycyrrhetinic acid. Biochem Biophys Res Commun1986, 134 (1), 29–36. [PubMed: 3947327]
29. Sezgin E; Kaiser H-J; Baumgart T; Schwille P; Simons K; Levental I, Elucidating membrane structure and protein behavior using giant plasma membrane vesicles. Nature Protocols2012, 7, 1042. [PubMed: 22555243]
30. Levental KR; Levental I, Isolation of Giant Plasma Membrane Vesicles for Evaluation of Plasma Membrane Structure and Protein Partitioning. In Methods in Membrane Lipids, Owen DM, Ed. Springer New York: New York, NY, 2015; pp 65–77.
31. Zhao C; Busch DJ; Vershel CP; Stachowiak JC, Multifunctional Transmembrane Protein Ligands for Cell-Specific Targeting of Plasma Membrane-Derived Vesicles. Small2016, 12 (28), 3837–48. [PubMed: 27294846]
32. Lopez W; Ramachandran J; Alsamarah A; Luo Y; Harris AL; Contreras JE, Mechanism of gating by calcium in connexin hemichannels. Proc Natl Acad Sci U S A2016, 113 (49), E7986–e7995. [PubMed: 27872296]
33. Gadok AK; Zhao C; Meriwether AI; Ferrati S; Rowley TG; Zoldan J; Smyth HDC; Stachowiak JC, The Display of Single-Domain Antibodies on the Surfaces of Connectosomes Enables Gap Junction-Mediated Drug Delivery to Specific Cell Populations. Biochemistry2018, 57 (1), 81–90. [PubMed: 28829120]
34. Motlagh NSH; Parvin P; Ghasemi F; Atyabi F, Fluorescence properties of several chemotherapy drugs: doxorubicin, paclitaxel and bleomycin. In Biomed Opt Express, 2016; Vol. 7, pp 2400–6. [PubMed: 27375954]
35. Barenholz Y; Amselem S; Goren D; Cohen R; Gelvan D; Samuni A; Golden Elisabeth B; Gabizon A, Stability of liposomal doxorubicin formulations: Problems and prospects. Medicinal Research Reviews1993, 13 (4), 449–491. [PubMed: 8361255]
36. Fritze A; Hens F; Kimpfler A; Schubert R; Peschka-Süss R, Remote loading of doxorubicin into liposomes driven by a transmembrane phosphate gradient. Biochimica et Biophysica Acta (BBA) - Biomembranes2006, 1758 (10), 1633–1640. [PubMed: 16887094]
37. Tacar O; Sriamornsak P; Dass CR, Doxorubicin: an update on anticancer molecular action, toxicity and novel drug delivery systems. J Pharm Pharmacol2013, 65 (2), 157–70. [PubMed: 23278683]
38. Dunlap SM; Chiao LJ; Nogueira L; Usary J; Perou CM; Varticovski L; Hursting SD, Dietary energy balance modulates epithelial-to-mesenchymal transition and tumor progression in murine claudin-low and basal-like mammary tumor models. Cancer Prev Res (Phila)2012, 5 (7), 930–42. [PubMed: 22588949]
39. Hilmer SN; Cogger VC; Muller M; Le Couteur DG, The hepatic pharmacokinetics of doxorubicin and liposomal doxorubicin. Drug Metab Dispos2004, 32 (8), 794–9. [PubMed: 15258103]
40. Li B; Xu H; Li Z; Yao M; Xie M; Shen H; Shen S; Wang X; Jin Y, Bypassing multidrug resistance in human breast cancer cells with lipid/polymer particle assemblies. Int J Nanomedicine2012, 7, 187–97. [PubMed: 22275834]

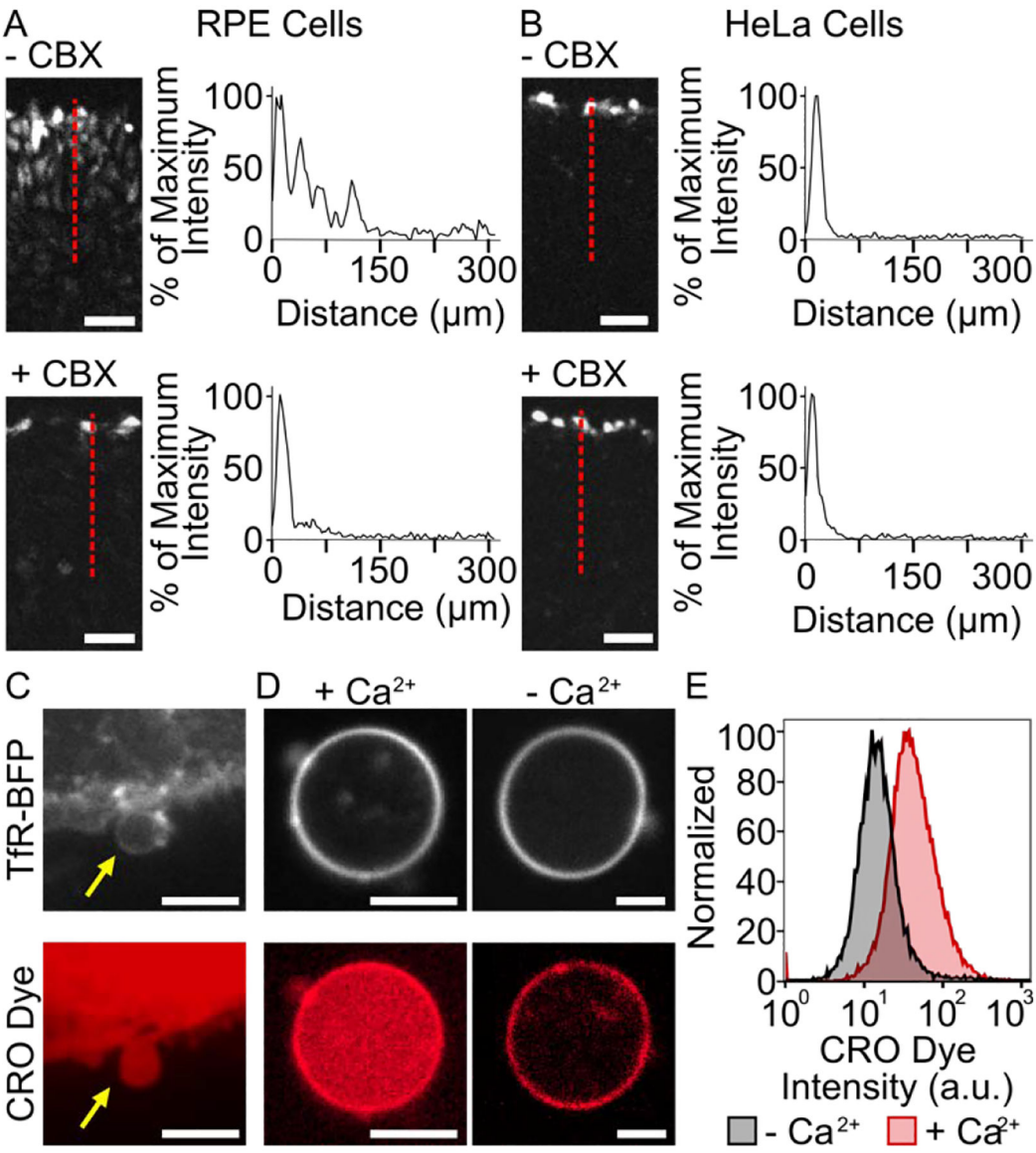

Figure 1.

Characterization of Connectosome donor cells. Functional gap junctions between RPE donor cells (A) and HeLa cells (B) are evaluated based on lucifer yellow CH dye transport in a scratch loading assay. Cells were scratched in the absence and presence of 100 μM carbenoxolone (CBX) gap junction inhibitor. An intensity profile along the red dotted line indicates dye spreading. Scale bars indicate 50 μm. (C) Connectosomes can be extracted from RPE cells by a cellular membrane blebbing process and loaded with molecular dye molecules such as calcein red-orange (CRO) acetomethoxy (AM) dye. Scale bars indicate 10 μm. (D) Connectosomes retain CRO dye in the presence of calcium ions and release dye when calcium ions are removed by 5 mM of EDTA and EGTA as chelators. Upon removal of CRO dye from the lumen, the fluorescence of the dye is still visible in the membrane, most likely due to non-specific interactions of amphiphilic dye molecules with

the membrane. Scale bars indicate 5 μm. (E) Flow cytometry histograms quantify CRO dye release from at least 10,000 connectosomes.

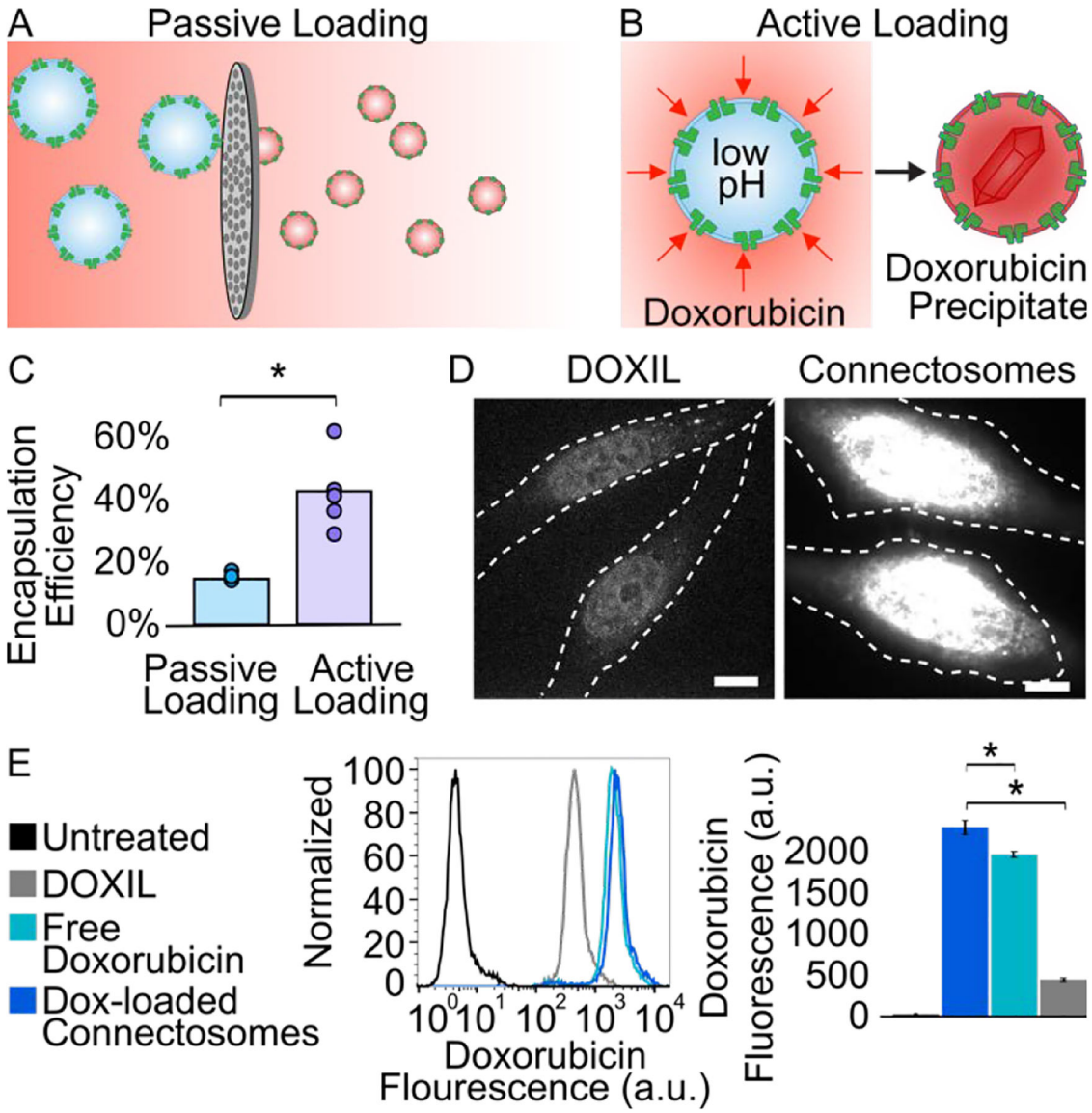

Figure 2.

Doxorubicin-loaded Connectosomes and *in vitro* delivery to cells. (A) A schematic of passive loading of doxorubicin into Connectosomes by extrusion in a solution of doxorubicin. (B) A schematic of active loading of doxorubicin into Connectosomes by a transmembrane ammonium sulfate gradient, which drives precipitation of doxorubicin inside of vesicles. (C) A chart comparing encapsulation efficiency from passive loading and active loading. Bars indicate the mean encapsulation efficiency. A two-tailed *t*-test indicates $p < 0.05$. (D) Representative confocal fluorescence microscopy images of HeLa cells incubated for 2 h with 12 μg of doxorubicin in DOXIL or in Connectosomes. The dashed white lines outline the cells. Scale bars indicate 10 μm. (E) Flow cytometry histograms of doxorubicin fluorescence within HeLa cells after two-hour treatment with DOXIL, free doxorubicin, and doxorubicin-loaded Connectosomes. Median doxorubicin fluorescence

intensity is quantified based on flow cytometry histograms. Error bars indicate standard deviation among three replicates. A two-tailed *t*-test indicates $p < 0.05$.

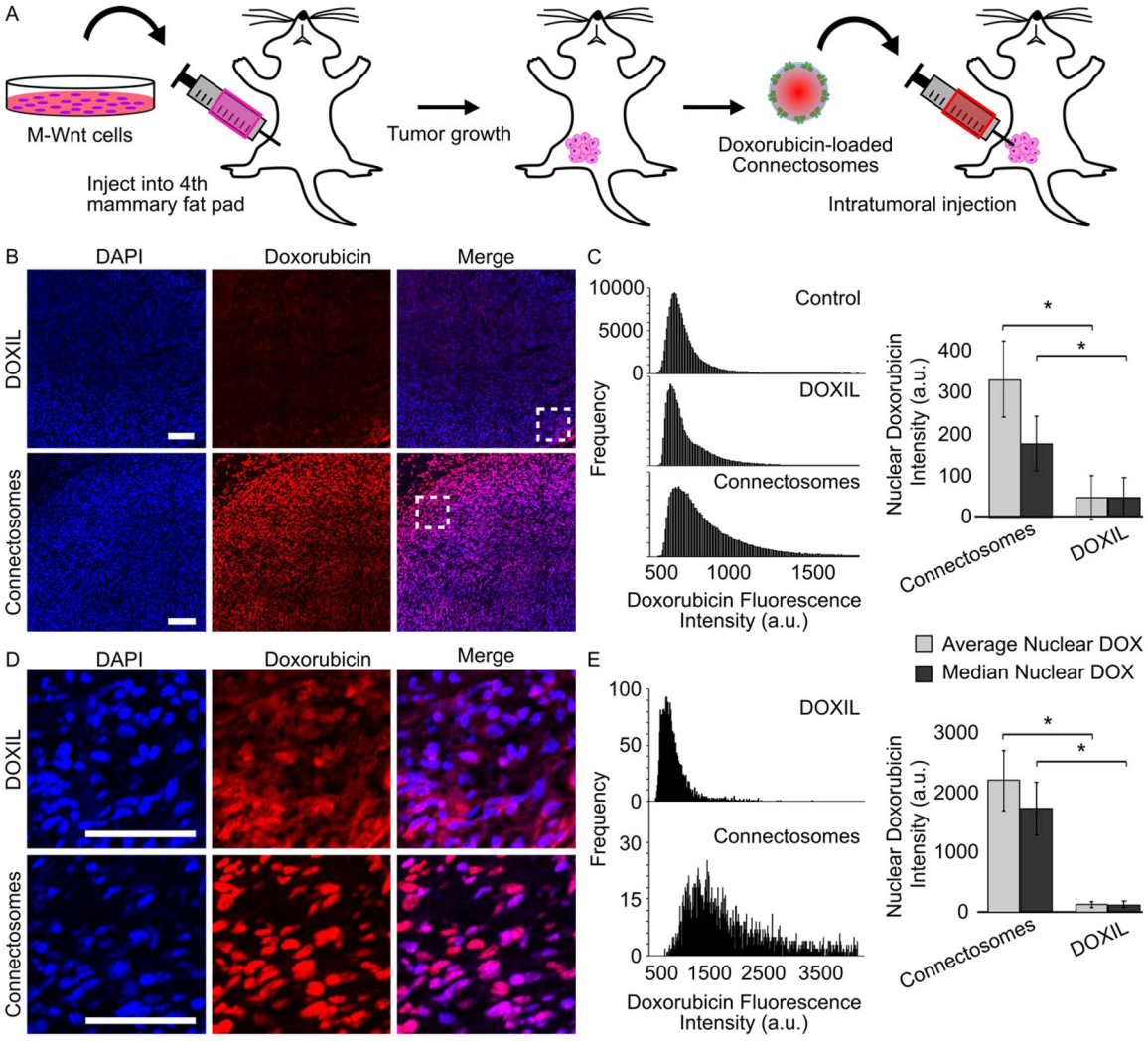

Figure 3.

Intracellular delivery of doxorubicin to orthotopic mammary tumors in mouse models. (A) A schematic of the *in vivo* experimental process. M-Wnt cells were injected into the fourth mammary fat pad of nine mice at a 1×10^6 cells/mouse to establish tumors. After tumors reached 4 – 7 mm in diameter, doxorubicin-loaded Connectosomes and DOXIL, each at 0.5 mg/kg, were injected directly into the tumors (n = 3). A third group of mice (n = 3) was left untreated. Mice were sacrificed 2 hours post intratumoral injection and tumors were analyzed. (B) Representative confocal fluorescence microscopy images of tumor sections after intratumoral injections of DOXIL and Connectosomes. DAPI staining was performed to visualize tumor cell nuclei. All images are adjusted to the same contrast settings and scale bars indicate 100 μm. (C) The nuclear doxorubicin fluorescence intensities from each entire tumor were plotted as histograms, and a bar chart quantifies the average nuclear doxorubicin intensity (light gray bar) and the median nuclear doxorubicin intensity (dark gray bar). Error bars indicate standard error of the mean, and a two-tailed *t*-test indicates $p < 0.05$. (D) Enlarged confocal microscopy images from the insets in (B) provide a closer view of nuclear doxorubicin fluorescence. (E) The nuclear doxorubicin fluorescence intensities from the

brightest region within each tumor were plotted as histograms, and a bar chart quantifies the average nuclear doxorubicin intensity (light gray bar) and the median nuclear doxorubicin intensity (dark gray bar). Error bars indicate standard error of the mean, and a two tailed-*t*-test indicates $p < 0.05$.